Renormalization-group study of the coupled XY-Ising models

Mai Suan Li* and Marek Cieplak
Institute of Physics, Polish Academy of Sciences, 02-668 Warsaw, Poland
(Received 17 August 1993; revised manuscript received 17 November 1993)

The coupled and discretized XY-Ising models describing frustrated XY and Josephson-junction systems are studied by the discretized Migdal-Kadanoff renormalization-group approach. Both uniform and disordered systems are considered. The phase diagram of the uniform two-dimensional ($2D$) model generally agrees with the previous studies but existence of a new antiferromagnetic phase is predicted. The random-gauge XY-Ising model is introduced to describe two-dimensional disordered systems with a half-integer number of the average flux per plaquette. Finite-temperature reentrancy from the paramagnetic to ferromagnetic Ising phases is predicted for the $2D$ random-gauge systems. At $T=0$, the gauge glass and Ising spin-glass phases can coexist provided the coupling to the Ising degrees of freedom is less than a critical value. In the $3D$ case, the finite-temperature gauge glass phase can exist only provided the Ising subsystem is also ordered, either in the ferromagnetic or the spin-glass fashion. The chaotic behavior of two mixed phases (one of them is of gauge glass and Ising spin glass and the other one is of gauge glass and Ising ferromagnet) is studied at $T=0$. Within the discretization scheme the Lyapunov exponents are found to be different for these phases.

I. INTRODUCTION

Two-dimensional Josephson junction arrays placed in a magnetic field have been a subject of extensive experimental[1-3] and theoretical[4-15] research. Models used to describe the physics of such arrays are typically derived from the XY Hamiltonian in which direction of a two-component spin is meant to represent phase ϕ_i of a wave function of an ith superconducting grain. Furthermore, disorder in the grain placement may introduce a quenched phase shift into the effective interaction of the spins. Additional effective randomness arises when the external magnetic field applied to the system is spatially nonuniform. An average flux per plaquette f_0 can in particular take half-integer values. If this happens, and if the disorder is positional in nature, then according to Granato and Kosterlitz,[9] the physics of the system may be captured by the random-gauge XY-Ising (RGXYI) model in which Ising and continuous degrees of freedom interact. The corresponding Hamiltonian is given by[9]

$$H=-J\sum_{\langle ij\rangle}(1+S_iS_j)\cos(\phi_i-\phi_j-A_{ij})-G\sum_{\langle ij\rangle}S_iS_j\ . \tag{1}$$

The coupling of strength J in Eq. (1) relates to the XY degrees of freedom and is restricted to neighboring grains. G is an interaction between the Ising variables $S_i=\pm1$. Granato and Kosterlitz[9] have considered the case in which A_{ij} are peaked in a Gaussian fashion around 0. In this paper, we consider the case of a strong disorder when the random quenched gauge field A_{ij} is taken to be uniformly distributed in the interval $[0,2\pi]$. We study the phase diagrams, scaling properties and nonuniversal chaotic behavior of the two-dimensional (2D) and 3D RGXYI models in an approximation in which ϕ_i take q discrete values, $q=2,3,\ldots\infty$, as explained in Sec. III.

The ramifications of this model will be described in more detail in Sec. II. Here, we note that the uniform version of the 2D model, described by the Hamiltonian

$$H=-J\sum_{\langle ij\rangle}(1+S_iS_j)\cos(\phi_i-\phi_j)-G\sum_{\langle ij\rangle}S_iS_j\ , \tag{2}$$

has been already studied by Monte Carlo simulations[10] and by a Migdal-Kadanoff renormalization-group (MKRG) scheme[8] (see Ref. 16 for MKRG) based on a Fourier series analysis for the XY spin degrees of freedom.[17] Our approach, described in Sec. III, is based on the MKRG scheme combined with the recently introduced discretization method of decimation[18] for the XY spins. We consider G to be non-negative, for simplicity and better focus.

As described in Sec. IV, our method yields a phase diagram as shown in Fig. 1 where various phases correspond to existence of a long-range order, or lack of it, in the XY and Ising subsystems. The topology of this phase diagram generally agrees with the previous studies[8,10] except that earlier studies did not indicate transition to the antiferromagnetic Ising arrangement at large negative G. We took the length rescaling factor b to be equal to 3 to be able to detect this transition.

The discretized MKRG applied to the 2D RGXYI model yields a phase diagram shown in Fig. 2. For $T\neq0$ the XY degrees of freedom do not produce any long-range order and the transition line shown in Fig. 2 refers to the Ising spins making a transition to a ferromagnetic ordering. One interesting aspect here is that the MKRG scheme predicts a *reentrant* behavior: cooling the system with G between $G_1\approx0.45$ and $G_c\approx0.55$ yields paramagnetic, ferromagnetic, and again paramagnetic Ising phases sequentially. The phase diagram at $T=0$ is more complicated since the XY spins form the gauge glass phase for any value of G whereas the Ising spins make a

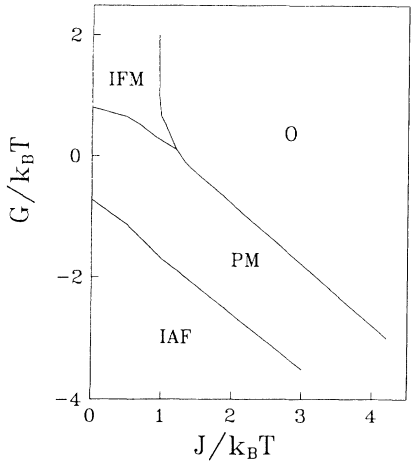

FIG. 1. The phase diagram of the uniform XY-Ising model (2) obtained by the discretized MKRG scheme. The length rescaling factor $b=3$ and the number of clock states $q=100$. There are four phases: Ising ferromagnetic ordered and XY disordered (IFM), Ising ferromagnetic and XY ordered (O), Ising and XY disordered (PM), and Ising antiferromagnetic ordered and XY disordered (IAF). The fully frustrated XY model corresponds to the line $G=0$.

spin-glass phase for $G<G_c$. Both of the amorphous long-range orders disappear at any infinitesimal temperature. But in 3D systems the glassy phases will be shown to extend to finite T (see Fig. 3).

The zero-temperature scaling exponents are discussed in Sec. V. For $G<G_c$ the gauge and Ising spin glasses coexist and the corresponding exponents for XY (y_{XY}) and Ising couplings (y_I) are found to be the same ($y_{XY}=y_I=y$). Similar to the gauge glass case[18] y is found not to depend on the number of clock states. In 2D the exponent y is the same for the Ising spin-glass (ISG) and RGXYI model, $y\approx -0.24$. This value is higher than the corresponding $y\approx -0.36$ found by the same method for the random-gauge XY (RGXY) model.[18] In the 3D case,

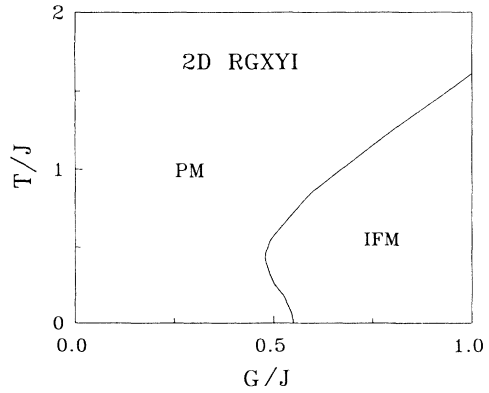

FIG. 2. The $T/J-G/J$ phase diagram for 2D RGXYI model, $q=100$, $N_p=2000$. Paramagnetic and Ising ferromagnetic phase are denoted by PM and IFM, respectively. At $T=0$ the gauge and Ising spin glasses coexist for $G<G_c$ ($G_c\approx 0.55J$) and for $G>G_c$ we have the gauge glass phase and Ising ferromagnetic order.

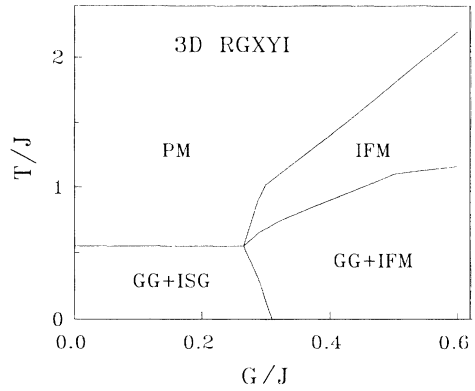

FIG. 3. The $T/J-G/J$ phase diagram for 3D RGXYI model, $q=100$, $N_p=2000$. We have four phases: PM, IFM, the mixed phase of gauge glass and Ising spin glass (GG+ISG), and the mixed phase of gauge glass and Ising ferromagnetic order (GG+IFM). The multicritical point corresponds to $T/J\approx 0.55$ and $G/J\approx 0.27$. For $0.27<G/J<0.31$ one can observe the reentrancy from the (GG+IFM) phase to the less ordered (GG+ISG) phase.

on the other hand, the RGXYI, RGXY, and ISG models all have the same exponent $y\approx 0.26$ within the discretization approximation. The equality of the exponents most likely reflect shortcomings of the scheme (see the discussion in Ref. 18).

One of the interesting properties of the spin-glass phase is its chaotic nature.[19–23] This means that the equilibrium spin configuration is unstable against arbitrarily weak modification of the exchange couplings or against any slight change in temperature.[21–23] Studies of chaos in Ising,[21–23] Heisenberg[24] spin glasses and gauge glass[25] show that the Lyapunov exponent ζ controlling routes to chaos does not depend on D. In Sec.VI we study chaos in the RGXYI model (1). The interplay between the continuous and discrete degrees of freedom gives rise to an interesting behavior. The discretization scheme yields ζ depending on q, similar to what was found in Ref. 25. The values of ζ in the mixed phase of gauge glass and Ising spin glass (GG+ISG) are found to be bigger than those in the mixed phase of gauge glass and Ising ferromagnet (GG+IFM). So the RGXYI model is an interesting example of a model in which the chaotic behavior is not universal.

The coupled XY Ising models allow one to study coexistence of different kinds of long-range orders and it is hoped that they will find applications outside the realm of the Josephson-junction arrays as well.

II. THE RGXYI HAMILTONIAN AND RELATED MODELS

Whenever variations in the amplitude of the wave function for an array of superconducting grains can be considered to be of secondary importance compared to the phase, the valid Hamiltonian is generally accepted to be given by[26]

$$H=-J\sum_{\langle ij\rangle}\cos(\phi_i-\phi_j-a_{ij})\ . \tag{3}$$

The gauge factor a_{ij} is equal to $(2\pi/\Phi_0)\int_i^j \mathbf{A}\cdot d\mathbf{l}$, where $\Phi_0=hc/2e$ is the flux quantum and $\mathbf{A}$ is the vector potential. The number of flux quanta per elementary plaquette is defined by $f=(1/2\pi)\sum a_{ij}$, where the sum is taken around the plaquette. If f is equal to $\frac{1}{2}$ the model reduces to the fully frustrated XY model which is described by the Hamiltonian

$$H=-\sum_{\langle ij\rangle} J_{ij}\cos(\phi_i-\phi_j)\ , \tag{4}$$

where $J_{ij}=\pm J$ satisfy the "odd" rule in which the number of bonds with negative J_{ij} in an elementary plaquette is odd.[13] On the other hand, when the gauge factor a_{ij} is assumed to be distributed uniformly between 0 and 2π, which corresponds to the situation with strong positional disorder and strong field, model (3) becomes a random-gauge XY (RGXY) model.[27] The RGXY model is believed to capture the essential physics of the vortex (or gauge) glass phase[27,28] in high-T_c materials.

Recently, Granato and Kosterlitz[9] have considered effects of disorder in Josephson-junction arrays in which f varies randomly in space. The average value of f will be denoted by f_0. The disorder may be introduced via the gauge factor $a_{ij}=a_{ij}^0+2\pi f_0 t_{ij}$, where $\sum a_{ij}^0=2\pi f_0$ and t_{ij} is an independent random variable. Using a Coulomb-gas representation and assuming disorder to be positional in character one can demonstrate[9] that for half-integer f_0 the original XY model (3) may be mapped to the RGXYI model of Eq. (1), where $A_{ij}=2\pi f_0 t_{ij}$. The Ising degrees of freedom reflect the existence of a domain-wall created by discrete charges[9,13] arising in the Coulomb-gas representation.

It should be noted that when the flux per plaquette is random one can consider $\delta f_R=f_0\sum t_{ij}$ to be an independent variable.[9] For the case of positional disorder Granato and Kosterlitz[9] have chosen t_{ij} in the following form:

$$t_{ij}=\mathbf{z}\cdot(\mathbf{r}_i-\mathbf{r}_j)\times(\mathbf{u}_i-\mathbf{u}_j)/2a_0^2\ . \tag{5}$$

Here a_0 is a lattice spacing and $\mathbf{z}$ is a unit vector perpendicular to the xy plane. Granato and Kosterlitz have assumed that the distribution of the random displacement of a grain $\mathbf{u}$ from its average position $\mathbf{r}$ is Gaussian

$$P(\mathbf{u})\propto\exp(-\mathbf{u}^2/2\Delta)\ , \tag{6}$$

which leads to a Gaussian distributed form of A_{ij}. The prediction for this case is[9] that one should observe a reentrancy from the Ising-ordered but XY-disordered phase or from the Ising and XY-disordered phase to the Ising-ordered and XY-ordered (i.e., superconducting) phase on the $T-\Delta$ phase diagram from the 2D version of the model. A similar reentrancy from a paramagnet to a ferromagnet has been proposed for the 2DXY model with a random Dzyaloshinskii-Moriya anisotropy.[29,30] This is not suprising because the latter model is a special case of model (3).

In this paper we consider the case of a strong disorder, i.e., the gauge factor $A_{ij}=2\pi f_0 t_{ij}$ in Eq. (3) (the relation between A_{ij} and a_{ij} is given above) is assumed to be distributed uniformly between 0 and 2π. In fact, in order to satisfy the condition that the average flux per plaquette is equal to f_0 the gauge factor A_{ij} should be assumed to take values restricted to the interval $[-\pi,\pi]$. However, due to the periodicity of the cosine function these conditions are equivalent. In this case model (3) reduces to the RGXYI model (1). One can see that RGXYI and RGXY 2D models correspond to the half-integer and integer values of the average numbers of flux quanta per plaquette, respectively. Similar to the RGXY model the RGXYI model may have some relevance to the gauge glass state in high-T_c materials and its study might prove to be useful in this context.

III. THE DISCRETIZED MKRG SCHEME

The MKRG transformation involves bond moving and decimations of the resulting 1D pieces of the lattice.[16] The procedure is generally exact for hierarchically constructed lattices in which each bond is replaced by b^{D-1} bonds, where b is the length rescaling factor. The simplest way to do the decimation step in the MKRG transformation for the RGXYI model (1) would be expected to be based on the harmonic approximation. In this approach the Hamiltonian is expanded about the equilibrium angle between neighboring XY spins up to quadratic terms with the Gaussian form of the partition function taken to be valid over the entire range of angles. In the presence of Ising degrees of freedom, however, such a simple scheme does not work, since the form of the Hamiltonian is not preserved under decimation. Discretization of the XY spins,[18] on the other hand, allows one to do the decimation step self-consistently and need not be restricted to the zero-temperature situation.

We begin by considering a more general Hamiltonian given by

$$H=-\sum_{\langle ij\rangle}(J_{ij}+K_{ij}S_iS_j)\cos(\phi_i-\phi_j-A_{ij})-\sum_{\langle ij\rangle}G_{ij}S_iS_j\ . \tag{7}$$

The RGXYI model may be obtained from the Hamiltonian (7) setting $J_{ij}=K_{ij}=J$ and $G_{ij}=G$.

The idea of the discretization is simple:[18] instead of allowing ϕ to be a continuous variable, we allow it to take one of q values which are uniformly distributed between 0 and 2π. The Hamiltonian is now defined for values of ϕ restricted to be $2\pi k/q$, where $k=0,1,2,\ldots,(q-1)$. We define

$$J_{ij}(q,k)=J_{ij}\cos(2\pi k/q-A_{ij})\ , \tag{8}$$

$$K_{ij}(q,k)=K_{ij}\cos(2\pi k/q-A_{ij})\ . \tag{9}$$

We find that

$$J_{ij}(q,q+m)=J_{ij}(q,m)\ ,\quad K_{ij}(q,q,+m)=K_{ij}(q,m)\ , \tag{10}$$

and

$$\sum_{k=0}^{q-1}J_{ij}(q,k)=0\ ,\quad \sum_{k=0}^{q-1}K_{ij}(q,k)=0\ . \tag{11}$$

The recursion relation for the discretized clock model involving also Ising degrees of freedom can be derived straightforwardly. We consider the cases with the rescaling factor $b=2$ and $b=3$ separately in the subsections below. It should be noted that under certain conditions the discretized Hamiltonian (7) is related to the chiral Potts model. These conditions are discussed in Appendix A.

A. The $b=2$ case

The recursion relations are based on a decimation procedure. For a scale factor b, $(b+1)$ spins in series are considered and a decimation is carried out to eliminate all the internal degrees of freedom. To obtain the rescaled coupling b^{D-1} such decimated bonds are added in parallel (see Ref. 18 for more details). In the $b=2$ case when spin 2 is decimated from a row containing spins 1, 2, and 3, one obtains

$$J'_{13}(q,k)=\frac{k_BT}{2}\left\{\ln[E(q,k)F(q,k)]-\frac{1}{q}\sum_{l=0}^{q-1}\ln[E(q,l)F(q,l)]\right\}, \tag{12}$$

$$K'_{13}(q,k)=\frac{k_BT}{2}\left\{\ln[E(q,k)/F(q,k)]-\frac{1}{q}\sum_{l=0}^{q-1}\ln[E(q,l)/F(q,l)]\right\}, \tag{13}$$

$$G'_{13}=\frac{k_BT}{2q}\sum_{l=0}^{q-1}\ln[E(q,l)/F(q,l)], \tag{14}$$

where

$$E(q,k)=\sum_{l=0}^{q-1}(\exp\{G_{12}+G_{23}+J_{12}[q,\mathrm{mod}(q+k-l,q)]+K_{12}[q,\mathrm{mod}(q+k-1,q)]+J_{23}(q,l)+K_{23}(q,l)\}$$
$$+\exp\{-J_{12}-J_{23}+J_{12}[q,\mathrm{mod}(q+k-l,q)]-K_{12}[q,\mathrm{mod}(q+k-1,q)]+J_{23}(q,l)-K_{23}(q,l)\}), \tag{15}$$

$$F(q,k)=\sum_{l=0}^{q-1}(\exp\{G_{12}-G_{23}+J_{12}[q,\mathrm{mod}(q+k-l,q)]+K_{12}[q,\mathrm{mod}(q+k-l,q)]+J_{23}(q,l)-K_{23}(q,l)\}$$
$$+\exp\{-J_{12}+J_{23}+J_{12}[q,\mathrm{mod}(q+k-l,q)]-K_{12}[q,\mathrm{mod}(q+k-l,q)]+J_{23}(q,l)+K_{23}(q,l)\}). \tag{16}$$

Equations (12)–(16) are derived by noting that the renormalized Hamiltonian is characterized by renormalized exchange interactions and by a constant term. The latter was determined by imposing condition (11) on the rescaled couplings.

B. The $b=3$ case

In order to obtain the phase diagram of the uniform XY-Ising model (2) either with the negative XY coupling J or with the negative Ising couplings G one has to take b to be equal to 3 since the decimation with $b=2$ makes antiferromagnetic couplings immediately become ferromagnetic. The recursion relations for the couplings J'_{14}, K'_{14}, and G'_{14} now arise from the decimation of two sites (spins 2 and 3 are decimated from a row containing spins 1, 2, 3, and 4) and their form remains the same as those given by Eqs. (12)–(14) for J'_{13}, K'_{13}, and G'_{13} in the $b=2$ case. However, the functions $E(q,k)$ and $F(q,k)$ become more complicated and are defined in Appendix B. The recursion scheme is completed by combining b^{D-1} bonds decimated according to (12)–(14) into one rescaled bond. The couplings $J_{ij}(q,k)$ and $K_{ij}(q,k)$ are q-valued variables.

IV. PHASE DIAGRAMS

We have tested our MKRG scheme on the uniform 2D XY-Ising model (2) by determining the corresponding phase diagram on the plane of variables G/k_BT and J/k_BT. One can show that in this case the microscopic and renormalized $J(q,k)$ have a positive maximum at $k=0$ and a negative minimum at $k=q/2$ (clock angle ϕ equal to 0 and π, respectively). Thus, phase diagram may be obtained by considering scaling of $J(q,0)$ and of G. As mentioned in the Introduction such a phase diagram has been already studied[8,10] but the existence of an antiferromagnetic Ising phase without XY order has not been indicated. Our result obtained for $q=100$ using the recursion relations (12)–(14) and (B1)–(B2) $(b=3)$ is shown in Fig. 1. We find that there are four possible phases: Ising ferromagnetic order and no XY order (IFM), ferromagnetic Ising and Kosterlitz-Thouless-like XY order (O), paramagnetic phase in both subsystems (PM), and antiferromagnetic Ising order with paramagnetic XY spins (IAF). The couplings $J(q,0)$ and G scale in these phases in the following way:

(i) $J(q,0)\to 0, G\to 0$: PM,
(ii) $J(q,0)\to 0, G\to\infty$: IFM,
(iii) $J(q,0)\to 0, G\to-\infty$: IAF,
(iv) $J(q,0)$-scale invariant, $G\to\infty$: O.

It should be noted that for 2D the MKRG approach cannot rigorously reproduce the quasi-long-range XY (Kosterlitz-Thouless-type) order.[17,18] The scale invariance is merely approximate in this method. In practice, a phase is declared to be the O phase if the scale invariance of $J(q,0)$ persists for about 20 iterations. Further itera-

tions lead to an eventual decrease of $J(q,0)$.

Note that the IAF phase occurs for large negative Ising coupling G with J still being positive. The topology of the phase diagram is like that obtained by Monte Carlo[10] and Fourier-based version of the MKRG (Ref. 8) method plus the extra IAF phase. These results suggest that the XY order is possible only if the Ising spins are ordered ferromagnetically.

Granato, Kosterlitz, and Lee[10] have found a Monte Carlo-based evidence for the existence of the first-order transition on the line separating the O and PM phases at large G. Furthermore, the so-called central charge has been shown[10] to vary continuously along the second-order portion of this line (the central charge is important in 2D conformal field theories[31] and it can be defined through the scaling behavior of the free energy for XY models).[32] Unfortunately, due to limited number of iterations possible for $b=3$ case, we are not able to check these interesting results.

We now turn to the analysis of the phase diagram of the 2D RGXYI model (1). We consider non-negative values of the Ising coupling ($G \geq 0$) which allow us to use the discretized scheme with the scaling factor $b=2$. The quenched random angle A_{ij} is chosen from the set of q values. The RGXYI model is believed to be obtained in the $q \to \infty$ limit. Following Ref. 18 to study the phase diagram it is sufficient to monitor scaling properties of the maximum (as a function of k) and minimum values of $J(q,k)$ averaged over the pool of N_p couplings. For instance

$$J_{\max}^{(n)} = \frac{1}{N_p} \sum_{i=1}^{N_p} \max J_i(q,k) \ . \tag{17}$$

Here, n denotes the iteration stage. One can show that the scaling of the average maximal and minimal $J(q,k)$ is identical, so we focus on the former [the average extremal values of the coupling $K(q,k)$ scale similar to those for $J(q,k)$].

It should be noted that the Ising coupling G is initially uniform but randomness in A_{ij} makes the effective G also random. Thus the nature of the Ising order can be characterized by the mean $\langle G_{ij} \rangle$ and dispersion σ_G of G_{ij} [$\sigma_G = (\langle G_{ij}^2 \rangle - \langle G_{ij} \rangle^2)^{1/2}$]. Our calculations follow the procedures described in Refs. 18 and 22. For RGXYI model we construct three pools for couplings $J_{ij}(q,k)$, $K_{ij}(q,k)$, and G_{ij} resulting from the random choices in the gauge factors A_{ij}. They are chosen initially to represent the Hamiltonian (1). Each of these pools is of N_p bonds and we consider N_p typically between 2000 and 5000. b^D members of each pool are chosen randomly to construct one renormalized coupling—this procedure is repeated until a renormalized pool is formed.

In the 2D case our results obtained for $q=100$ and $N_p=2000$ are shown in Fig. 2. The line separating disordered and Ising ferromagnetic ordered phases is obtained by the scale invariance of the mean of the Ising couplings. The PM and IFM phases are identified as follows:

(i) $J_{\max}^{(n)} \to 0, \langle G_{ij} \rangle \to 0, \sigma_G \to 0$: PM,

(ii) $J_{\max}^{(n)} \to 0, \langle G_{ij} \rangle \to \infty, \sigma_G / \langle G_{ij} \rangle \to 0$: IFM.

At $T \neq 0$ neither the gauge (XY) glass nor the Ising spin glass are stable. In other words, similar to the RGXY model, the RGXYI model does not display a truly superconducting phase in two dimensions at $T \neq 0$. Such a behavior has been recently found in experiments on $YBa_2Cu_3O_{7-\delta}$ thin films[33] but it is difficult to estimate what average flux per plaquette would correspond to these experimental situations. It is very interesting that one can observe the paramagnet-ferromagnet-paramagnet reentrancy for $0.48 < G < G_c$, where $G_c \approx 0.55J$. At $T=0$ the effect of randomness in the gauge factor A_{ij} on the Ising couplings is so strong that we have the phase where gauge and Ising spin glasses coexist for $G < G_c$. For $T=0$ and $G > G_c$ the gauge glass phase coexists with the Ising ferromagnetic one. In the next section we will show that G_c depends on the number of clock states q but the dependence saturates already at $q=10$ for $D=2$.

Establishing the order of the paramagnetic-ferromagnetic phase transition shown in Fig. 2 would require a calculation of the thermal exponent y_T. In our case y_T can be determined from the flow of the mean of the Ising couplings $\langle G_{ij} \rangle$ at temperatures very close to the critical T_c, i.e., $\langle G_{ij} \rangle (T_c - \delta T) - \langle G_{ij} \rangle (T_c) \sim L^{y_T}$. If $y_T = D$ the transition should be first order.[34] Taking $\delta T / T_c$ of order 10^{-2} the exponent y_T is found to be independent of G, and equal to 0.89 ± 0.04. Since y_T is smaller than the spatial dimension of 2 the paramagnetic-ferromagnetic transition in 2D RGXYI should be continuous.

We discuss now the $T/J - G/J$ phase diagram for 3D RGXYI model. The results obtained for $q=100$ and $N_p=2000$ are shown in Fig. 3. In three-dimensions the Ising spin-glass and gauge glass phases can exist at $T \neq 0$. There are four phases: PM, IFM, the mixed (GG+ISG), and (GG+IFM) phases. The definitions of the PM and IFM phases are the same as those for the 2D case of the RGXYI model. In the mixed phases the scaling behavior of $J_{\max}^{(n)}$, $\langle G_{ij} \rangle$, and σ_G is as follows:

(i) $\sigma_G \to \infty, \langle G_{ij} \rangle / \sigma_G \to 0, J_{\max}^{(n)} \to \infty$: (GG+ISG) ,

(ii) $\langle G_{ij} \rangle \to \infty, \sigma_G / \langle G_{ij} \rangle \to 0, J_{\max}^{(n)} \to \infty$: (GG+IFM) .

The PM-(IFM+GG) line obtained from the scale invariance of $J_{\max}^{(n)}$ and σ_G is parallel to the G/J axis. The (GG+IFM)-IFM boundary is found by the scale invariance of $J_{\max}^{(n)}$ but the mean of Ising couplings increases under iteration. The PM-IFM transition is defined by the scale invariance of the mean of the Ising couplings. The multicritical point where four phases meet corresponds to $T_c \approx 0.55$ and $G_c/J \approx 0.27$. In the narrow interval $0.27 < G/J < 0.31$ the discretization scheme suggests that on lowering temperature the system can pass PM-IFM-(GG+IFM)-(GG+ISG) phases. It should be noted that the gauge glass phase can coexist only either with the ISG with the IFM order, and no evidence for coexistence of ISG and long-range Ising ordering is seen. The phase diagram is meant to be schematic and, in particular, the order of the transition lines remains to be determined.

V. SCALING PROPERTIES OF THE RGXYI MODEL

In this section we study the scaling properties of the RGXYI model using the discretized scheme with

$b=2$ ($G\geq 0$). In the gauge glass phase the maximal $J(q,k)$ would obey a power law, i.e., $J_{\max}^{(n)}\sim b^{ny_{XY}}$, $L=b^n$, where y_{XY} is a $T=0$ scaling exponent for the couplings J_{ij}. The Ising spin-glass phase is characterized by the exponent y_I, where $\sigma_G\sim L^{y_I}$.

At $T=0$ and G smaller than some critical value $G_c(q)$, which depends on the number of clock states q, the effect of randomness in A_{ij} on the Ising coupling is so strong that one can observe the coexistence of the gauge (XY) and Ising spin-glass in 2D and 3D [in 2D (3D) the gauge glass phase means that the average extremum value of $J(q,k)$ scales down (up) according to a power law]. The dependence of $G_c(q)$ is substantial at small values of q, as shown in Fig. 4, but it saturates at 0.55 and 0.31 for 2D and 3D systems, respectively. Above $G_c(q)$ the Ising ferromagnetic order coexists with the gauge glass phase.

The upper part of Fig. 5 shows the scaling of $J_{\max}^{(n)}$ for selected values of q in 2D for $G=0$. Obviously, within the discretized scheme the exponent y_{XY} does not depend on the number of clock states and is almost the same as that for the 2D Ising Gaussian spin glass obtained by the MKRG method. One can show also that y_{XY} is independent of the Ising coupling G. The $q=2$ case is found to be special. For the scaling factor $b=2$ and $D=2J_{\max}^{(n)}$ scales down exponentially for $G=0$ but a power law is seen for $G\neq 0$ (see the lower part of Fig. 5, a similar behavior may be observed for the dispersion of Ising couplings σ_G). Figure 5 shows that y_{XY} does not depend on G for $q=2$. This conclusion is found to be valid for any q and for y_I. Figure 6 shows that σ_G scales like $J_{\max}^{(n)}$. Thus, within the discretization approximation we use $y_{XY}=y_I=y\approx -0.24$ for the 2D RGXYI system. This value is higher than the corresponding value $y\approx -0.36$ for the RGXY model.[18]

We now turn to the 3D generalization of the model. The $T=0$ scaling exponent y in $D=3$ is found in our discretized MKRG scheme to be the same for the RGXYI (similar to the $D=2$ case $y_{XY}=y_I=y$ and y is independent of G), RGXY, and Ising Gaussian spin-glass models (see Fig. 7). Its value is equal to $y=0.26$. This should be compared to the exponent y of 0.19 obtained by the transfer-matrix method for the 3D Ising spin glasses[35–37] and y of order 0.3 for the RGXY model obtained by the method of $T=0$ quenches based on 300 samples.[38] The defect-wall renormalization-group calculation based on larger statics[39] and extensive Monte Carlo simulations[40] suggest, however, that $y\approx 0.05$ for the 3D RGXY model. It should be interesting to estimate y for the RGXYI model by these methods.

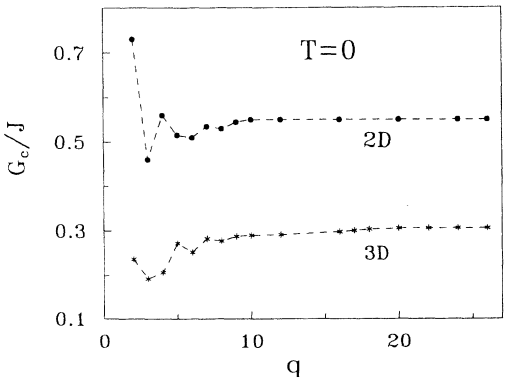

FIG. 4. The dependence of the critical value $G_c(q)$ on q for 2D and 3D. The number of couplings in the pool, N_p, is equal to 2000. The dashed lines are a guide for eyes. At $T=0$ the gauge and spin-glass phases coexist for $G<G_c(q)$. For $4G>G_c(q)$ we have the gauge glass phase with Ising ferromagnetic order. $G_c(q)$ seems to saturate at $0.55J$ ($q\geq 10$) and at $0.31J$ ($q\geq 18$) for 2D and 3D, respectively.

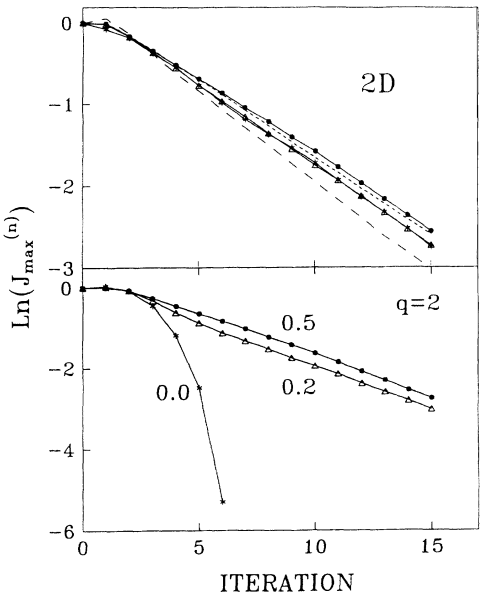

FIG. 5. Scaling of $J_{\max}^{(n)}$ for the RGXYI model for $D=2$, $G=0$, $q>2$, and $T=0$ (upper part). The dotted and dashed lines corresponds to the Ising Gaussian spin glass and RGXY model (with $q=100$), respectively. The data points are for the RGXYI model with various values of q: 3 (stars); 6 (open triangles); and 12 (closed circles). The exponent $y\approx -0.24$ for RGXYI and Ising Gaussian spin-glass models whereas $y\approx -0.36$ for the RGXY model. The scaling of $J_{\max}^{(n)}$ for $D=2$, $q=2$, and $T=0$ is shown in the lower part. The values of G are indicated in the plot. For nonzero G one has a power law with the same slope.

VI. CHAOS IN THE RGXYI MODEL

As mentioned in the Introduction the spin-glass phase is unstable against arbitrarily weak perturbations in the exchange couplings. Using a simple Imry-Ma argument[41] one can show that routes to chaos are controlled by the Lyapunov exponent $\zeta=d_s/2-y$, where d_s is the interfacial entropy exponent,[21] which in the Ising case can also be interpreted as a fractal dimension of the droplet surface. The chaotic nature associated with the flipping of large droplets of Ising spins has been invoked to interpret dynamical spin-glass experiments involving aging[20] and dimensional crossover[42] in layered systems and as a probe of conductance fluctuation in mesoscopic metallic glasses.[43]

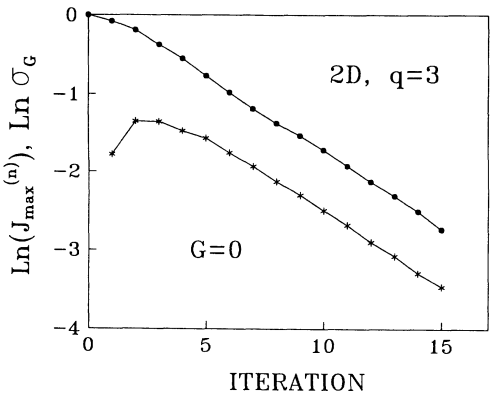

FIG. 6. Scaling of $J_{\max}^{(n)}$ (closed circles) and σ_G (stars) for $D=2$, $q=3$, and $G=0$. Obviously, at large scales these two curves have the same slope providing $y_{XY}=y_I$.

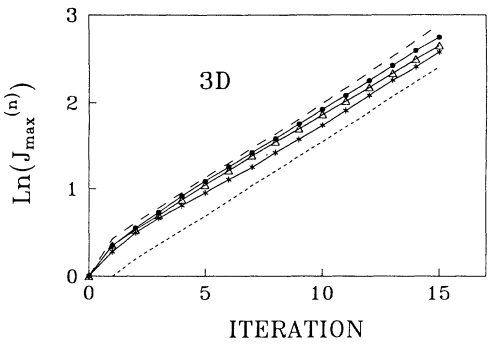

FIG. 7. Same as in the upper part of the Fig. 5 but for $D=3$. $y\approx 0.26$ for RGXY, RGXYI, and Ising Gaussian spin-glass models.

The chaotic nature has been also observed for the systems with continuous symmetry such as vector spin[24] and gauge glasses.[25] Using the discretization MKRG scheme one can show that the Lyapunov exponent of the RGXY model varies with the number of clock states reflecting the nonuniversal behavior of the interfacial entropy. It should be noted that chaos in the critical region in three-dimensional Ising[23] and RGXY (Ref. 44) systems is characterized by a new critical exponent leading to new scaling laws. In this section we will show that chaotic behavior of the RGXYI system is much richer compared to spin and gauge glasses. Since the glass state does not exist in the 2D RGXYI model at $T\neq 0$ we will focus on the chaos at $T=0$.

In order to study chaos at $T=0$ we consider two pools $\{J_i(q,k)\}$ and $\{J_i'(q,k)\}$ that initially differ from each other by a tiny amount at fixed values of the uniform Ising couplings G. For $G<G_c$ the Ising spin and gauge glass phases coexist, both the XY and Ising spin configurations, therefore, should be sensitive in a small change of couplings. The corresponding Lyapunov exponents ζ_{XY} and ζ_I are obtained by considering how the distances between couplings in these pools diverges with the size of the system until they become decorrelated completely. The characteristic mean square distances are defined as follows:[21,22,25]

$$d_{XY}^2(n)=\sum_{i=1}^{N_q}\sum_{k=0}^{q-1}[J_i(q,k)-J_i'(q,k)]^2\Big/\sum_{i=1}^{N_q}\sum_{k=0}^{q-1}[J_i(q,k)+J_i'(q,k)]^2\ , \tag{18}$$

$$d_I^2(n)=\sum_{i=1}^{N_q}(G_i-G_i')^2\Big/\sum_{i=1}^{N_q}(G_i+G_i')^2\ . \tag{19}$$

The distance $d_{XY}^2(n)$ and $d_I^2(n)$ approach 1 (corresponding to a fully chaotic phase) with a power-law dependence on the length scale L, $d_{XY}^2(n)\sim L^{2\zeta_{XY}}$ and $d_I^2(n)\sim L^{2\zeta_I}$.

For $G>G_c$ there is no Ising spin-glass order in the 2D RGXYI model and then it is sufficient to determine only ζ_{XY}. One can demonstrate that within the discretized approximation we use $\zeta_{XY}=\zeta_I$ for given values of q and G ($G<G_c$). So, in what follows we will focus only on $d_{XY}^2(n)$ and ζ_{XY}, and notation XY in these expressions will be omitted.

We first study chaos in the (GG+ISG) phase ($G<G_c$). A plot of d^2 versus n is shown in Fig. 8 and Fig. 9 for selected values of q ($G/J=0.1$) and for $D=2$ and $D=3$, respectively. The curves in each plot have different slopes meaning that the corresponding Lyapunov exponents ζ are different for different q. Within the error bar of order ± 0.02 the values of exponent ζ are the same for $D=2$ and $D=3$. The scaling of d^2 for 2D, $q=2$ and $G/J=0.1$ and 0.5 is shown in Fig. 10. Clearly, these two curves have the same slope suggesting ζ in the (GG+ISG) phase does not depend on the Ising interaction.

We turn now to the discussion of chaos in the (GG+IFM) phase ($G>G_c$). Similar to the (GG+ISG) phase ζ may be shown to be independent of D and G but varies with q. For a given value of q the values of ζ are, however, different for (GG+ISG) and (GG+IFM) phases. This is illustrated in Fig. 11, where the scaling of d^2 for these phases is plotted ($D=2, q=3$).

So similar to the gauge glass case[25,44] ζ depends on the number of clock states q. The values of ζ(GG+ISG) and ζ(GG+IFM) are shown in Fig. 12. The numerical data for them are described by the fit $\zeta(\mathrm{GG+ISG})=1.1-0.404\exp(-0.345q)$ and $\zeta(\mathrm{GG+IFM})=1-0.403\exp(-0.355q)$. At large q the exponent ζ(GG+ISG) saturates at 1 which is the same for the RGXY model. For small q and within the error bar of order ± 0.04 the Lyapunov exponent of the (GG+IFM)

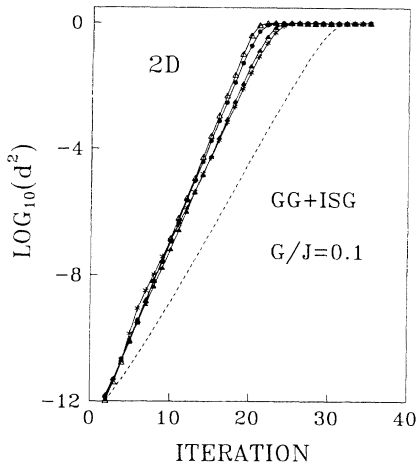

FIG. 8. Scaling of the normalized distance between two pools for $D=2$ $G=0.1J$ [the (GG+ISG)-phase] and selected values of q. The pool contains 5000 couplings. The chaos is induced by a perturbation in couplings J_{ij} of magnitude $10^{-6}J$. For $q=2$ (stars), 3 (closed triangles), 6 (closed circles), and 12 (open triangle) we find $\zeta=0.91$, 0.98, 1.05, and 1.09, respectively. The dotted line corresponds to the ISG case with $\zeta=0.74$. The error bars are of order ± 0.02.

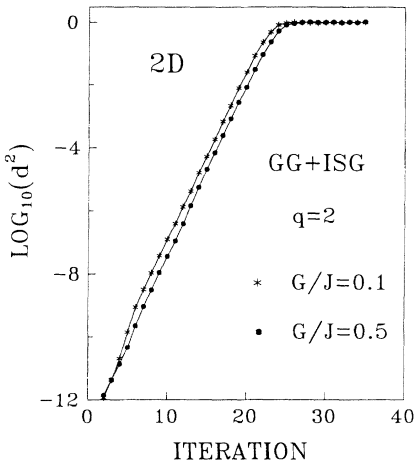

FIG. 10. The scaling of d^2 for $D=2$, $q=2$, $G=0.1J$, and $G=0.5J$. Clearly for given values of G the chaotic exponent ζ of the (GG+ISG) phase does not depend on G. For this set of parameters we have $\zeta \approx 0.91$ and the error bar is of order ± 0.02. The pool contains 5000 couplings.

phase in the RGXYI model coincide with that for the gauge glass phase in the RGXY one. This conclusion may be understood in a following way. In the (GG+IFM) phase one has Ising order so that ϕ is controlled by an effective Hamiltonian

$$H_{\text{eff}} = -\tilde{J} \sum_{\langle ij \rangle} \cos(\phi_i - \phi_j - A_{ij}) , \tag{20}$$

where $\tilde{J}=J(1+\langle S_i \rangle^2)$. H_{eff} is just a Hamiltonian of the RGXY model.

VII. CONCLUSION

We have introduced the RGXYI model which may capture physics of 2D Josephson-junction systems when the average flux per plaquette is half-integer. The MKRG scheme predicts a reentrancy phenomenon for this model. It should be worthwhile to check this result by more exact approaches. The chaotic behavior of the RGXYI model is found to be very interesting: the Lyapunov exponent is different for (GG+ISG) and (GG+IFM) phases.

It is known[28] that the existence of the gauge glass phase in 2D at $T=0$ substantially changes dynamics of the system at $T \neq 0$. For example, the temperature dependence of the nonlinear current density is described by a power law predicted by the scaling theory for 2D gauge glass.[28] On the other hand, at small G one can observe coexistence of the gauge and Ising spin glasses at $T=0$ in the 2D RGXYI model. It would be interesting to find

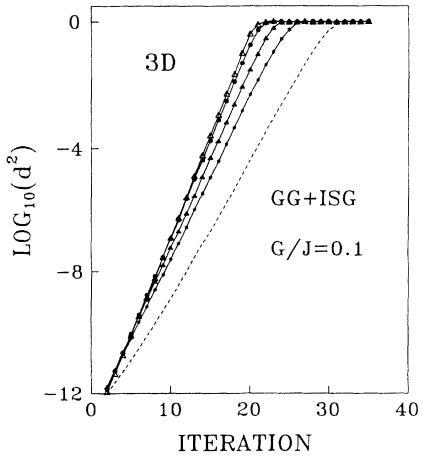

FIG. 9. Same as in Fig. 8 but for $D=3$. Within the error bars of order ± 0.02 the values of ζ coincide with those for two dimensions. The pool consists of 5000 couplings.

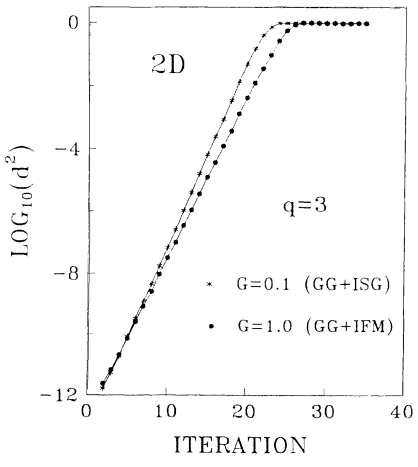

FIG. 11. Scaling of d^2 for $D=2$, $q=3$. The curves have different slopes meaning that the Lyapunov exponent is different for the (GG+ISG) ($G=0.1J<G_c$, $\zeta=0.86$, stars) and (GG+IFM) ($G=J>G_c$, $\zeta=0.77$, closed circles) phases. The critical value G_c for 2D and $q=3$ is equal $G_c=0.46J$.

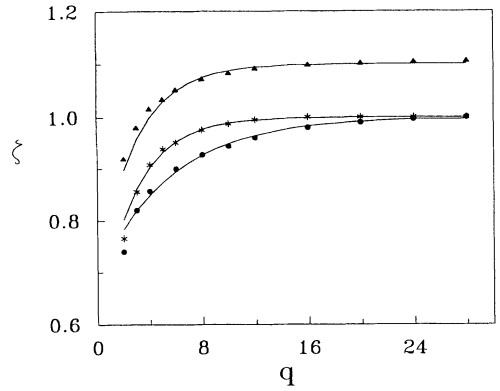

FIG. 12. The dependence of ζ for (GG+ISG) (closed triangles) and for (GG+IFM) phases (stars) on q in the RGXYI model. The solid curves correspond to the fit $\zeta(\mathrm{GG}+\mathrm{ISG})=1.1-0.404\exp(-0.345q)$ and $\zeta(\mathrm{GG}+\mathrm{IFM})=1-0.403\exp(-0.355q)$. The closed circles correspond to ζ for the gauge glass in the RGXY model (Ref. 25) with the fit $\zeta(\mathrm{GG})=1-0.309\exp(-0.18q)$.

out whether the existence of the ISG phase affects scaling predictions for dynamics properties of the gauge glass in this model.

ACKNOWLEDGMENTS

Discussions with Jayanth R. Banavar are highly appreciated. Support from the Polish Agency KBN (Grant No. 2-0462-91-01) is acknowledged.

APPENDIX A

Here, we comment on the relationship of the discretized model (7) to the Q-state chiral Potts model described by the Hamiltonian[45]

$$H=-J\sum_{\langle ij\rangle}\cos\left[\frac{2\pi}{Q}(k_i-k_j)-\Delta_{ij}\right], \tag{A1}$$

where $k_i=0,1,\ldots,Q-1$ are the spin state variables and Δ_{ij} is a position dependent variable. Consider the discretized version of Hamiltonian (7) where the order of discretization is q. If

$$G_{ij}=\tilde{G}_{ij}\cos A_{ij}\ , \tag{A2}$$

then model (7) may be mapped to different clock models depending on whether q is odd or even. In the case of odd q, following Ref. 46 model (7) may be mapped to the following $2q$-state model:

$$H=-\sum_{\langle ij\rangle}J'(k_i-k_j)\cos\left[\frac{2\pi}{2q}(k_i-k_j)-A_{ij}\right], \tag{A3}$$

where $k=0,1,\ldots,2q-1$. Couplings J' are effectively state dependent and given by

$$J'_{ij}(k)=\begin{cases}K_{ij}+J_{ij}+\tilde{G}_{ij}\ , & k=0\\ K_{ij}+J_{ij}\ , & k \text{ even}\\ K_{ij}+\tilde{G}_{ij}\ , & k=q\\ K_{ij}\ , & k \text{ odd and } \neq q\ .\end{cases} \tag{A4}$$

It is only in the limit of $J_{ij}=\tilde{G}_{ij}=0$ (but the phase shift A_{ij} is still nonzero) that the effective coupling J'_{ij} ceases to be state dependent. Then model (A3) reduces to the chiral Potts model (A1) with Δ_{ij} replaced by A_{ij} and $Q=2q$. The $q\to\infty$ limit of model (A3) with $J'_{ij}=J$ has been discussed in Ref. 18. RGXYI model (1) studied in this paper involves the uniform couplings $G_{ij}=G$ and $J_{ij}=K_{ij}=J$ and our results for odd q, therefore, do not relate to the chiral Potts model.

If q is even then model (7) may be mapped to the following q-state model:

$$H=-\sum_{\langle ij\rangle}J''(k_i-k_j)\cos\left[\frac{2\pi}{q}(k_i-k_j)-A_{ij}\right], \tag{A5}$$

where $k=0,1,\ldots,q-1$. Couplings J'' are state dependent and are given by

$$J''_{ij}(k)=\begin{cases}2K_{ij}+J_{ij}+\tilde{G}_{ij}\ , & k=0,q/2\\ 2K_{ij}+J_{ij}\ , & \text{otherwise}\ .\end{cases} \tag{A6}$$

In the limit of $\tilde{G}_{ij}=0$ the effective coupling J''_{ij} ceases to be state dependent and model (A5) reduces to the chiral Potts model (A1) with Δ_{ij} replaced by A_{ij} and $Q=q$. Thus our results on the phase diagrams for an even q and $G=0$ are related to the phase transitions in the chiral Potts model.

APPENDIX B

Expressions of $E(q,k)$ and $F(q,k)$ for the $b=3$ case are as follows:

$$\begin{aligned}E(q,k)=\sum_{l=0}^{q-1}\sum_{m=0}^{q-1}\big(&\exp\{G_{12}+G_{23}+J_{34}+G_{12}[q,\mathrm{mod}(k-l+q,q)]+K_{12}[q,\mathrm{mod}(k-l+q,q)]\\ &+J_{23}[q,\mathrm{mod}(l-m+q,q)]+K_{23}[q,\mathrm{mod}(l-m+q,q)]+J_{34}(q,m)+K_{34}(q,m)\}\\ &+\exp\{-G_{12}-G_{23}+G_{34}+J_{12}[q,\mathrm{mod}(k-l+q,q)]-K_{12}[q,\mathrm{mod}(k-l+q,q)]\\ &+J_{23}[q,\mathrm{mod}(l-m+q,q)]-K_{23}[q,\mathrm{mod}(l-m+q,q)]+J_{34}(q,m)+K_{34}(q,m)\}\\ &+\exp\{G_{12}-G_{23}-G_{34}+J_{12}[q,\mathrm{mod}(k-l+q,q)]+K_{12}[q,\mathrm{mod}(k-l+q,q)]\\ &+J_{23}[q,\mathrm{mod}(l-m+q,q)]-K_{23}[q,\mathrm{mod}(l-m+q,q)]+J_{34}(q,m)-K_{34}(q,m)\}\\ &+\exp\{-G_{12}+G_{23}-G_{34}+J_{12}[q,\mathrm{mod}(k-l+q,q)]-K_{12}[q,\mathrm{mod}(k-l+q,q)]\\ &+J_{23}[q,\mathrm{mod}(l-m+q,q)]+K_{23}[q,\mathrm{mod}(l-m+q,q)]+J_{34}(q,m)-K_{34}(q,m)\}\big)\ ,\end{aligned} \tag{B1}$$

$$F(q,k)=\sum_{l=0}^{q-1}\sum_{m=0}^{q-1}(\exp\{G_{12}-G_{23}+G_{34}+J_{12}[q,\mathrm{mod}(k-l+q,q)]+K_{12}[q,\mathrm{mod}(k-l+q,q)]$$
$$+J_{23}[q,\mathrm{mod}(l-m+q,q)]-K_{23}[q,\mathrm{mod}(l-m+q,q)]+J_{34}(q,m)+K_{34}(q,m)\}$$
$$+\exp\{-G_{12}+G_{23}+G_{34}+J_{12}[q,\mathrm{mod}(k-l+q,q)]-K_{12}[q,\mathrm{mod}(k-l+q,q)]$$
$$+J_{23}[q,\mathrm{mod}(l-m+q,q)]+K_{23}[q,\mathrm{mod}(l-m+q,q)]+J_{34}(q,m)+K_{34}(q,m)\}$$
$$+\exp\{G_{12}+G_{23}-G_{34}+J_{12}[q,\mathrm{mod}(k-l+q,q)]+K_{12}[q,\mathrm{mod}(k-l+q,q)]$$
$$+J_{23}[q,\mathrm{mod}(l-m+q,q)]+K_{23}[q,\mathrm{mod}(l-m+q,q)]+J_{34}(q,m)-K_{34}(q,m)\}$$
$$+\exp\{-G_{12}-G_{23}-G_{34}+J_{12}[q,\mathrm{mod}(k-l+q,q)]-K_{12}[q,\mathrm{mod}(k-l+q,q)]$$
$$+J_{23}[q,\mathrm{mod}(l-m+q,q)]-K_{23}[q,\mathrm{mod}(l-m+q,q)]+J_{34}(q,m)-K_{34}(q,m)\})\ . \quad \text{(B2)}$$

*On leave from Thai Nguyen Technical Institute, Vietnam.

[1]R. F. Voss and R. A. Webb, Phys. Rev. B **25**, 3446 (1982); R. A. Webb, R. F. Voss, G. Grinstein, and P. M. Horn, Phys. Rev. Lett. **51**, 690 (1983); B. J. van Wees, H. S. J. van der Zant, and J. E. Mooij, Phys. Rev. B **35**, 7291 (1987).

[2]M. Tinkham, D. W. Abraham, and C. J. Lobb, Phys. Rev. B **28**, 6578 (1983); D. Kimhi, F. Leyaz, and D. Ariosa, *ibid.* **29**, 1487 (1984); R. K. Brown and J. C. Garland, *ibid.* **33**, 7827 (1986); Ch. Leemann, Ph. Lerch, G. A. Racine, and P. Martinoli, Phys. Rev. Lett. **56**, 1291 (1986); J. P. Carini, Phys. Rev. B **38**, 63 (1988).

[3]M. G. Forrester, H. J. Lee, M. Tinkham, and C. J. Lobb, Jpn. J. Appl. Phys. **26**, 1423 (1987); Phys. Rev. B **37**, 5966 (1988); S. P. Benz, M. G. Forrester, M. Tinkham, and C. J. Lobb, *ibid.* **38**, 2869 (1988).

[4]M. Y. Choi and S. Doniach, Phys. Rev. B **31**, 4516 (1985); M. Y. Choi and D. Stroud, *ibid.* **32**, 5773 (1985).

[5]M. Yosefin and E. Domany, Phys. Rev. B **32**, 1778 (1985).

[6]E. Granato and J. M. Kosterlitz, J. Phys. C **19**, L59 (1986).

[7]E. Granato and J. M. Kosterlitz, Phys. Rev. B **33**, 4767 (1986).

[8]E. Granato, J. Phys. C **20**, L215 (1987).

[9]E. Granato and J. M. Kosterlitz, Phys. Rev. Lett. **62**, 823 (1989).

[10]E. Granato, J. M. Kosterlitz, and J. Lee, Phys. Rev. Lett. **66**, 1090 (1991).

[11]J. Lee, J. M. Kosterlitz, and E. Granato, Phys. Rev. B **43**, 11 531 (1991).

[12]B. Berge, H. T. Diep, A. Ghazali, and P. Lallemand, Phys. Rev. B **34**, 3177 (1986); W. Y. Shih and D. Stroud, *ibid.* **32**, 158 (1985); J. E. van Himbergen, *ibid.* **33**, 7857 (1986).

[13]T. C. Halsey, J. Phys. C **18**, 2437 (1985); Phys. Rev. B **31**, 5728 (1985); S. E. Korshunov and G. V. Uimin, J. Stat. Phys. **43**, 1 (1986).

[14]M. Y. Choi, J. S. Chung, and D. Stroud, Phys. Rev. B **35**, 1669 (1987); A. Chakrabarti and C. Dasgupta, *ibid.* **37**, 7557 (1988).

[15]M. Thijssen and H. J. F. Knops, Phys. Rev. B **37**, 7738 (1988).

[16]A. A. Migdal, Zh. Eksp. Teor. Fiz. **69**, 1457 (1975) [Sov. Phys. JETP **42**, 743 (1975)]; L. P. Kadanoff, Ann. Phys. (N.Y.) **100**, 359 (1976).

[17]J. V. Jose, L. P. Kadanoff, S. Kirkpatrick, and D. R. Nelson, Phys. Rev. B **16**, 1217 (1977).

[18]M. Cieplak, J. R. Banavar, M. S. Li, and A. Khurana, Phys. Rev. B **45**, 786 (1992).

[19]S. R. McKay, A. N. Berker, and S. Kirkpatrick, Phys. Rev. Lett. **48**, 767 (1982); J. Appl. Phys. **53**, 7976 (1982).

[20]D. S. Fisher and D. A. Huse, Phys. Rev. Lett. **56**, 1601 (1986); Phys. Rev. B **38**, 386 (1988).

[21]A. J. Bray and M. A. Moore, Phys. Rev. Lett. **58**, 57 (1987).

[22]J. R. Banavar and A. J. Bray, Phys. Rev. B **35**, 8888 (1987).

[23]M. Nifle and J. J. Hilhorst, Phys. Rev. Lett. **68**, 2992 (1992); Physica A **194**, 462 (1993).

[24]J. R. Banavar and A. J. Bray, Phys. Rev. B **38**, 2564 (1988).

[25]M. Cieplak, M. S. Li, and J. R. Banavar, Phys. Rev. B **47**, 5022 (1993).

[26]W. Y. Shih, C. Ebner, and D. Stroud, Phys. Rev. B **30**, 134 (1984); S. John and T. C. Lubensky, *ibid.* **34**, 4815 (1986).

[27]D. A. Huse and H. S. Seung, Phys. Rev. B **42**, 1059 (1990).

[28]M. P. A. Fisher, Phys. Rev. Lett. **62**, 1415 (1989); D. S. Fisher, M. P. A. Fisher, and D. A. Huse, Phys. Rev. B **43**, 130 (1991).

[29]M. Rubinstein, B. Shraimain, and D. R. Nelson, Phys. Rev. B **27**, 1880 (1983).

[30]M. Paczuski and M. Kadar, Phys. Rev. B **43**, 8331 (1991).

[31]D. Friedan, Z. Qiu, and S. Shenker, Phys. Rev. Lett. **52**, 1575 (1984); A. B. Zamolodchikov, Pis'ma Zh. Eksp. Teor. Fiz. **43**, 565 (1986) [JETP Lett. **43**, 730 (1986)].

[32]M. Thijssen and H. J. F. Knops, Phys. Rev. B **42**, 2438 (1990).

[33]C. Dekker, P. J. M. Wöltgens, R. H. Koch, B. W. Hussey, and A. Gupta, Phys. Rev. Lett. **69**, 2717 (1992).

[34]B. Nienhuis and M. Nauenberg, Phys. Rev. Lett. **35**, 477 (1975).

[35]A. J. Bray and M. A. Moore, in *Heidelberg Colloquium on Glassy Dynamics*, edited by L. Van Hemmen and I. Morgenstern (Springer, Berlin, 1987), p. 121.

[36]W. L. McMillan, Phys. Rev. B **30**, 476 (1984).

[37]M. Cieplak and J. R. Banavar, J. Phys. A **23**, 4385 (1990).

[38]M. Cieplak, J. R. Banavar, and A. Khurana, J. Phys. A **24**, L145 (1991).

[39]M. J. P. Gingras, Phys. Rev. B **45**, 7547 (1992).

[40]J. D. Reger, T. A. Tokuyasu, A. P. Young, and M. P. A. Fisher, Phys. Rev. B **44**, 7147 (1991).

[41]Y. Imry, S. K. Ma, Phys. Rev. Lett. **35**, 1399 (1975).

[42]P. Grangerb, J. Mattsson, P. Nordblad, L. Lundgren, R. Stubi, J. Bass, D. L. Leslie-Pelecky, and J. A. Cowen, Phys. Rev. B **44**, 4410 (1991).

[43]S. Feng, A. J. Bray, P. A. Lee, and M. A. Moore, Phys. Rev. B **36**, 5624 (1987); M. Cieplak, B. R. Bulka, and T. Dietl, *ibid.* **44**, 12 337 (1991).

[44]M. S. Li and M. Cieplak, Physica A **197**, 507 (1993).

[45]S. Ostlund, Phys. Rev. B **24**, 398 (1981); D. A. Huse, *ibid.* **24**, 5180 (1981); M. N. Barber, J. Phys. A **15**, 915 (1982).

[46]H. Au-Yang and J. H. Perk, Int. J. Mod. Phys. A **7**, Suppl. 1B, 1007 (1992).